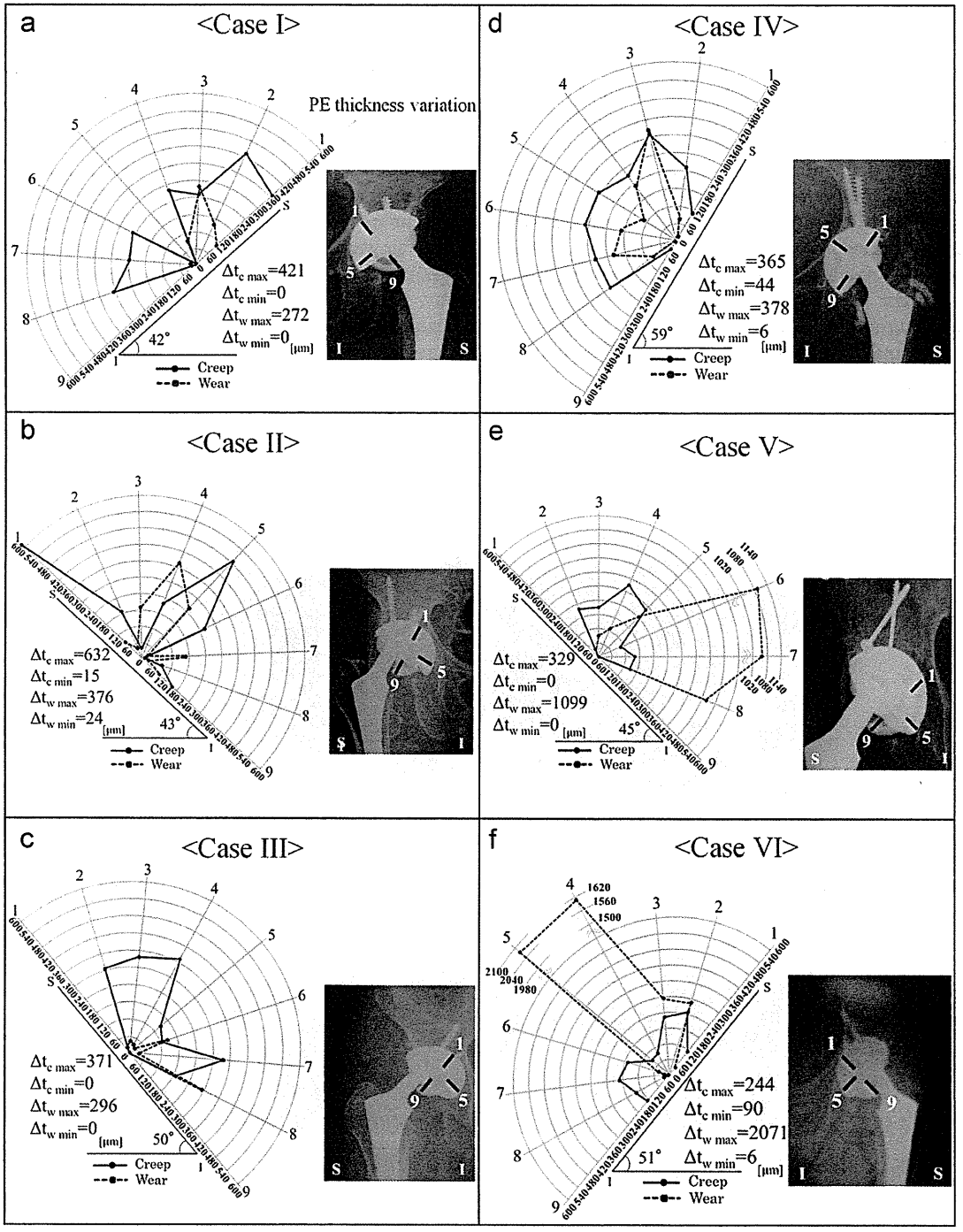

Fig. 4 – Polar plots of the total creep and wear displacements recorded along a circumferential path of the UHMWPE shell of the investigated implants. Inclination angles are also shown for better clarity. Radiographic analyses are shown as collected immediately before revision surgery. The numbers shown in inset of the radiographs correspond to the numbers locating the radial directions in each polar plot.

3. Results and discussion

3.1. *Phenomenology of the failure cases*

The photographs in Fig. 3(a)–(f) represent the ceramic-cup/polyethylene-shell components of the investigated failed implants after being retrieved from the patients' body. The results of radiographic examinations immediately before revision surgery are shown for each of the studied Cases in Fig. 4. Case I in Table 1 (Figs. 3 and 4(a)) was revised after dislodgment (namely a clearly visible shift of the joined ceramic/polyethylene parts out of the metal shell). The cause

Please cite this article as: Okita, S., et al., Failure analysis of sandwich-type ceramic-on-ceramic hip joints: A spectroscopic investigation into the role of the polyethylene shell component. Journal of the Mechanical Behavior of Biomedical Materials (2013), http://dx.doi.org/10.1016/j.jmbbm.2013.01.022

of failure was simply classified as "dislodgment", although the retrieval also showed a clear-cut circumferential fracture trajectory dividing the ceramic liner into two distinct parts of about the same size (cf. Fig. 3(a)). The two cases labeled II and III in Table 1 were revised due to liner dislodgment (cf. Fig. 3(b) and (c), respectively, with radiographic analyses in Fig. 4(b) and (c)), and showed no fracture of the ceramic liner. Among the remaining three cases, Case IV showed no visible dislodgment (Figs. 3 and 4(d) for Case IV), but its ceramic liner fractured with extensive fragmentation (cf. photograph of the broken pieces of the ceramic liner in inset of Fig. 3(d)). The many broken ceramic pieces needed to be retrieved separately from the implant in the body of the patient. Cases V and VI both underwent dislodgment (Fig. 3(e) and (f), respectively; radiographs shown in Fig. 4(e) and (f), respectively) and fracture of the respective ceramic liners. However, important differences could be noted in comparing the fracture patterns of the latter two ceramic liners as compared to the other fractured liners. Case V showed three broken (chipped) pieces at the rim of its ceramic liner, but unlike Case I no circumferential fracture path was observed. On the other hand, the fracture pattern in Case IV was somewhat merging the patterns found in Cases I and V, with the display of both edge chipping (into two pieces) and a main circumferential fracture path. The different fracture pattern represents an important difference, which most likely differentiates the mechanisms leading to the catastrophic failure events occurred *in vivo* in different implants, and which will be discussed in forthcoming Section 3.3. In all cases of dislodgment, we never observed any (even local) detachment between the UHMWPE shell and the ceramic liner. Both components thus shifted with remaining integer to each other. Except for Cases I and IV, the polyethylene shells showed significant damages, including severe abrasive wear especially localized at the rim area, in which significant residual deformation also locally occurred, possibly due to creep. In a purely mechanistic view, the damages appeared similar to those reported earlier by Messieh et al. (1994) in describing wear debris originated from the contact of a bipolar cup with the femoral neck. Some circumferential cracks were also visible near the edge of the polyethylene shell belonging to Cases V and VI. Cases II, III, and VI showed severe delamination and flaking of the polymeric structure mainly at the contact area between the shell and stem, but also in other zones around the circumference of the shell. Kaku et al. (2001) described phenomenologically similar microfracture events and damages for the polyethylene liner of a bipolar femoral head. Moreover, our data seem to confirm a thesis put forward by Yamaguchi et al. (2000) in reviewing a large number of acetabular components. These researchers found that cups with impingement were systematically more anteverted than those without impingement. As a matter of fact, we also found significant UHMWPE damage due to impingement in Cases IV and VI, which were the implants with the highest anteversion angle in the studied series of retrievals. Besides promoting subluxation and dislocation of the femoral head, prosthetic impingement was reported to significantly contribute to implant loosening by imparting eccentric loads to the cup and by the direct production of polyethylene wear debris (Coventry, 1985; McCollum and Gray, 1990; Woo and Morrey, 1982). We shall indeed show in the following sections that local impingement might have played a detrimental role also in sandwich-type implants by promoting sliding of the UHMWPE layer (always integer to the ceramic shell) and, thus, leading to the observed common dislodgment of the polyethylene and ceramic parts. As far as the inclination angle was concerned, it is conceivable to expect a higher creep deformation in the zone near the edge of the UHMWPE liner in the implants with high inclination angle.

3.2. *Creep and wear analyses of retrieved polyethylene shells*

Following the Raman confocal procedures described in Section 2.2, spatially resolved profiles of the strain field that permanently remained stored in the UHMWPE shells of the retrieved sandwich-type implants could be measured and displayed in polar plots as a function of sample depth along the entire thickness of the shells. Note (from Table 1) that the pristine thickness of the UHMWPE shell was different for different implants, despite all implants being from the same maker. An intermediate thickness of 3 mm (Cases I and VI), a minimum thickness of 2 mm (Cases IV and V) and a maximum thickness of 5 mm (Cases II and III) were the three patterns available in the examined retrievals. In Fig. 4, polar plots are shown, for each of the examined retrieval, of the total creep displacements recorded along a typical circumferential path of the UHMWPE shell. The examined circumferential path crossed the main wear zone of the bearing surfaces. Creep displacements could be obtained by numerically integrating over the entire thickness of the shell the respective in-depth strain profiles, according to a procedure explained in previous publications (Kumakura et al., 2009; Pezzotti et al., 2011). In-depth strain profiles were in turn non-destructively retrieved from FWHM data analyses of the Raman band of UHMWPE representing symmetric stretching of the C–C bonding. In the polar plots, the inclination angle of the acetabular cup of each implant is also represented for better clarity, as given in Table 1. It was already mentioned in Section 2.2 that the numerical integration, performed for calculating local creep displacements, encompassed profiles of fifty points for each polar angle, while data points at each depth represented an average value retrieved over 900 spectra. The thickness reductions that arose from creep deformation, Δt_c, and wear abrasion, Δt_w, as they piled up during the *in vivo* lifetime are represented in Fig. 4 by full and broken lines, respectively. Numerical values of both creep displacements and worn out thicknesses as measured at different locations in each retrieval are also explicitly listed for better clarity in Table 2. The Δt_w values were obtained by subtracting the measured, Δt_c, from the pristine cup thickness at each location of the polar plot. In the previous section, it was described that no detachment between the UHMWPE shell and the ceramic liner was observed in the investigated retrievals. Therefore, different from the usual definition of abrasive wear between ceramic and polyethylene bearings, the wear damages reported in this paper unequivocally refer to the occurrence of backside wear due to friction between the Ti-metal shell and the UHMWPE shell. A proof for this

Please cite this article as: Okita, S., et al., Failure analysis of sandwich-type ceramic-on-ceramic hip joints: A spectroscopic investigation into the role of the polyethylene shell component. Journal of the Mechanical Behavior of Biomedical Materials (2013), http://dx.doi.org/10.1016/j.jmbbm.2013.01.022

Table 2 – Numerical values of thickness reduction in six cases of UHMWPE shells as detected at different polar locations in the nominal main wear zone. Thickness reductions are differentiated into separated components due to creep and backside wear, the former ones obtained by Raman spectroscopic assessments.

Creep displacement, Δt_c [μm]

	Measurement point								
Case	1	2	3	4	5	6	7	8	9
I	362	421	256	275	0	250	241	316	0
II	632	185	41	223	484	249	15	80	156
III	0	304	344	371	160	124	344	180	0
IV	112	250	365	277	305	307	282	275	44
V	0	221	214	329	290	116	163	156	0
VI	118	244	214	99	90	178	187	149	120

Worn out thickness, Δt_w [μm]

	Measurement point								
Case	1	2	3	4	5	6	7	8	9
I	109	163	272	95	0	16	16	17	0
II	94	46	187	376	258	24	170	24	92
III	0	29	58	34	24	146	41	296	0
IV	6	79	378	233	137	189	227	103	15
V	0	29	96	121	240	1099	1052	504	0
VI	38	286	296	1614	2071	44	20	25	6

Please cite this article as: Okita, S., et al., Failure analysis of sandwich-type ceramic-on-ceramic hip joints: A spectroscopic investigation into the role of the polyethylene shell component. Journal of the Mechanical Behavior of Biomedical Materials (2013), http://dx.doi.org/10.1016/j.jmbbm.2013.01.022

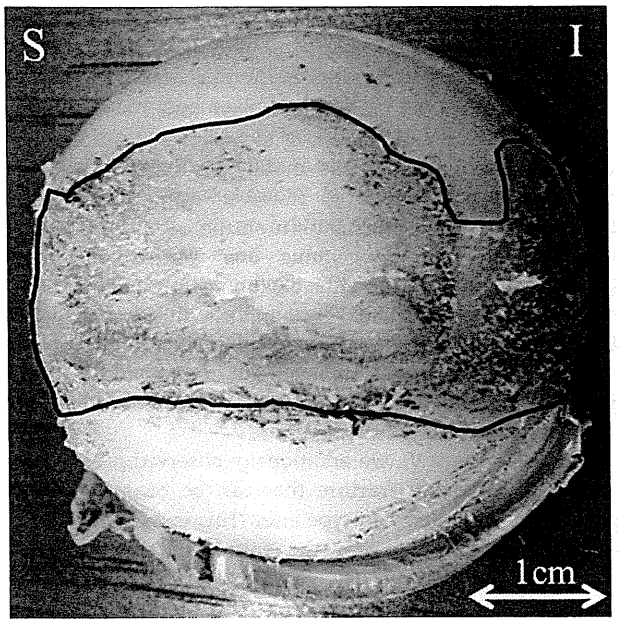

Fig. 5 – Evidence for backside wear in the polyethylene layer of Case V. The abraded area has been highlighted with a black contour for better visualization.

assertion is given in the photograph in Fig. 5. However, it is anticipated at the outset that a comprehensive interpretation of the data shown in Fig. 4 might be quite complex due to the fact that we could only access to final thickness variations, without the knowledge of the temporal sequence at which such variations occurred (i.e., in particular at which stage of dislodgment they occurred). Moreover, different implants showed quite different patterns of creep and wear damages in terms of the respective thickness reductions. Nevertheless, some important evidences could be collected, which can be summarized as follows:

(i) In comparing different retrievals, it immediately appears evident that the thickness reductions due to backside wear in Cases V and VI were exceptionally high as compared to the other retrievals examined. However, while in Case VI the maximum wear damage measured ($\Delta t_{w\ max}$=2.071 mm) occurred in correspondence of a location where one would approximately expect the occurrence of the main wear zone, in Case V the maximum wear damage ($\Delta t_{w\ max}$=1.099 mm) occurred at a location corresponding to what one would expect to be the non-wear zone of the cup at the time of implantation. Both implants indeed showed substantial dislodgment, but the difference in the observed locations of wear patterns suggest that, unlike Case VI, abrasive backside wear in the UHMWPE shells of Case V occurred after slip of the UHMWPE shell out of the Ti-alloy shell. This speculation is partly confirmed by the fact that in Case VI significant damage of the UHMWPE shell appeared in the rim area as a consequence of stem impingement during gait (after rotation of the ceramic/UHMWPE components inside the metal shell), while the shell in Case V showed no damage at its rim but it was severely abraded in its backside zone due to impingement on the edge of the metal cup after dislodgement (cf. Fig. 3).

(ii) Both Cases II and III, which by design incorporated the thickest UHMWPE component in their pristine state, showed significant abrasive damage at the rim of the UHMWPE shell (i.e., by impingement of the stem). The *in vivo* times of these two implants were nearly the same and also the longest in the studied series. Both implants showed pronounced dislodgment at the time of revision surgery, but no fracture of the ceramic cup. The occurrence of backside wear was quite limited and localized in both implants, suggesting that dislodgement occurred suddenly. However, peculiar to Case II was a quite high creep displacement at the upper edge of the UHMWPE shell, due to severe impingement by the femoral head at the onset angle for subluxation.

(iii) Case IV, which showed no dislocation and destruction of the ceramic liner, was the only implant in which creep deformation was quite homogeneous in the polar rotation interval encompassing gait motion (all other implants showed inhomogeneous distributions of creep displacements with maximum values at variable inclination angles). We shall associate the lack of localized deformation in the UHMWPE shell of Case IV to the absence of dislodgement. Despite being the implant with the shortest exposure *in vivo*, the implant of Case IV showed creep displacements comparable with those measured in the long-term retrievals analyzed. This observation confirms the notion that creep deformation in polyethylene hip components mainly occurs during the initial time (<2 yr) from primary surgery (Bewill et al., 2005; Glyn-Jones, 2008).

The results shown in Fig. 4 help visualizing a significant creep contribution to the *in vivo* penetration of ceramic liner component into the Ti-metal shell as a consequence of local flattening of the polyethylene shell. The general conclusion drawn from the examination of Δt_c data in comparison with the overall displacements, Δt, is that, at the time of explantation, the creep flattening contribution in the UHMWPE shell could be locally as large as one third of the entire UHMWPE shell thickness. Such large creep displacements were not only responsible for the linear penetration of the ceramic liner into the metal shell, but also for the successive patient weight redistribution with application of an asymmetric (incorrect) loading to the ceramic liner.

An interesting finding could be obtained by examining the residual strain profiles in Case VI, as developed along the subsurface of the UHMWPE layer of the retrievals. We examined the strain profiles developed at three characteristic zones; namely, the main wear zone, the non-wear zone, and the contact zone after dislodgement (labeled (1), (2), and (3), respectively in the draft of Fig. 2), which corresponded to the angular sectors labeled 3–4, 8–9, and 1–2 in Fig. 2(a), respectively. A low (and conspicuously constant) level of residual strain was found along the thickness, as expected, in the non-wear zone. Moreover, the magnitude of the total

Please cite this article as: Okita, S., et al., Failure analysis of sandwich-type ceramic-on-ceramic hip joints: A spectroscopic investigation into the role of the polyethylene shell component. Journal of the Mechanical Behavior of Biomedical Materials (2013), http://dx.doi.org/10.1016/j.jmbbm.2013.01.022

thickness reduction due to residual strain was similar in the main wear zone and in the contact zone after dislodgement (both in the order of the hundreds of μm; cf. Table 2). However, such thickness reduction arose from residual strain profiles with quite different morphologies. Fig. 6 shows a comparison among the three strain profiles mentioned above. In zone (1), a maximum was found at about 700 μm in the sub-surface, while in zone (3) the strain level was constant along the sub-surface. This interesting detail is in agreement with the previous studies of residual deformation in the polyethylene liner of conventional hip implants (Pezzotti et al., 2011) and suggests that the profile of residual strain piled up during *in vivo* cycling load, namely upon regular deambulation, can be differentiated in the experimental practice from that piled up under abnormal loading conditions (i.e., local impingement after liner dislodgement).

3.3. *Failure mechanisms in sandwich-type ceramic-on-ceramic implants*

In a recent paper, Dalla Pria et al. (2010) have reviewed the topic of breakage of ceramic-on-ceramic hip couples. Although none of the reviewed implants belonged to the sandwich-type studied here, extensive discussions and classifications were given of fracture patterns in ceramic liners, which present interesting aspects and provide guidance in the context of this paper. Two main types of fracture mode were reviewed: (i) the so-called "undetected fracture" of the liner, in which circumferential fracture occurred into two parts above the conical coupling, with no fragments (Sariali et al., 2009); and, (ii) the rim fragmentation (or chipping) fracture which arises from neck impingement against the rim of the ceramic liner upon subluxation (Ha et al., 2006; Willmann, 2001). The above-referred type (i) of fracture is quite unusual and was not observed in our investigation. In type (ii), even assuming the ceramic liner being correctly positioned in the metal shell, a combination of shocks and edge loading by the ceramic head was designated as responsible for rim breakage, which is indeed what we have observed in Cases V and VI (cf. Fig. 3(e) and (f)). Chipping of the liner has been reported to occur when the inclination angle is too steep or when the anteversion angle is out of the safe zone (Hasegawa et al., 2006; Widmer and Zurfluh, 2004; Willmann, 2001). This was obviously the case in retrieval Case VI, which showed both inclination and anteversion angles at the limit of the safe zone. On the other hand, in Case V, the cup was initially positioned in a correct way (cf. angles in Table 1). However, from the extensive backside abrasive damage pattern on the UHMWPE shell, we could deduce that the ceramic liner worked for a non-negligible period of time after having been rotated by about 45° into the metal shell (cf. Fig. 5 and the thickness reduction by wear in Fig. 4(e)), thus dramatically increasing the risk of subluxation and head impingement. It should be indeed assumed that after liner rotation had occurred did the rim chipping presumably happened.

In Cases I and VI, we additionally observed a completely different pattern of fracture that can be considered to be peculiar to the sandwich-type liner. This is a circumferential crack path spanning over the entire cup, which in turn resulted in splitting of the ceramic liner into two broken hemispheres (cf. Fig. 3(a) and (f)). In Case VI, this fracture pattern was additive to rim chipping. The origin of such different crack path has not yet been discussed in the published literature. We newly suggest here that it arose from localized loading (in bending) of the convex surface of the ceramic cup after its rotation into the metal shell. The effects on fracture paths of this kind of localized loading applied on the pole of a curved brittle system with unsupported margins has been studied in detail by Rudas et al. (2005) by means of a boundary element analysis. This analysis indeed predicted (and experimentally validated) the formation of cracks, which nucleated at the pole of the cup and extended toward the dome base. Fig. 7 shows a series of drafts that attempts to comprehensively describe the sequence of degradative events that led to the observed fracture patterns. Fig. 7(a) shows a hip joint correctly implanted, in which the body weight selectively induces creep deformation in a limited interval of radial angles in the UHMWPE shell (Fig. 7(b)). Under the effect of an increased tangential force due to the local deformation of the polyethylene shell, dislodgment eventually occurred

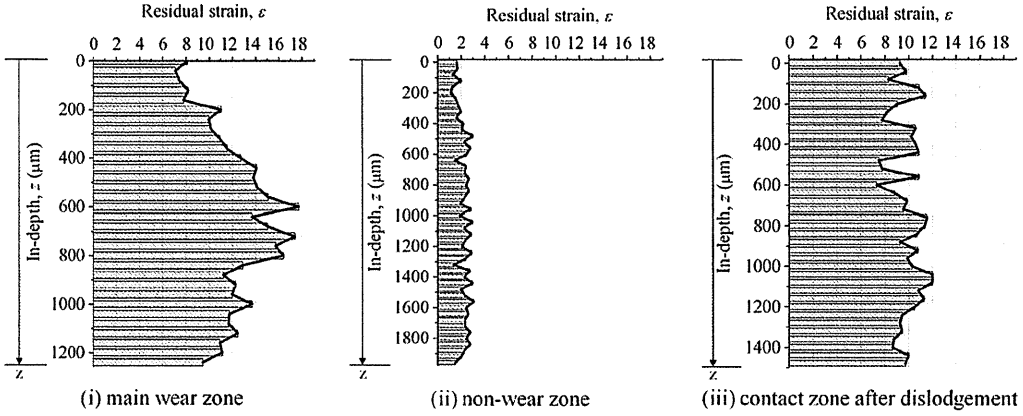

Fig. 6 – Profile of residual strain as detected along the sub-surface of the UHMWPE layer of Case VI in the main wear zone, the non-wear zone, and in the contact zone after dislodgment (labeled zone (1), (2), and (3), respectively, in Fig. 2(a)). Note that the zero point of the in-depth abscissa correspond to the side of the UHMWPE layer in contact with the ceramic liner, as shown in Fig. 2(b).

Please cite this article as: Okita, S., et al., Failure analysis of sandwich-type ceramic-on-ceramic hip joints: A spectroscopic investigation into the role of the polyethylene shell component. Journal of the Mechanical Behavior of Biomedical Materials (2013), http://dx.doi.org/10.1016/j.jmbbm.2013.01.022

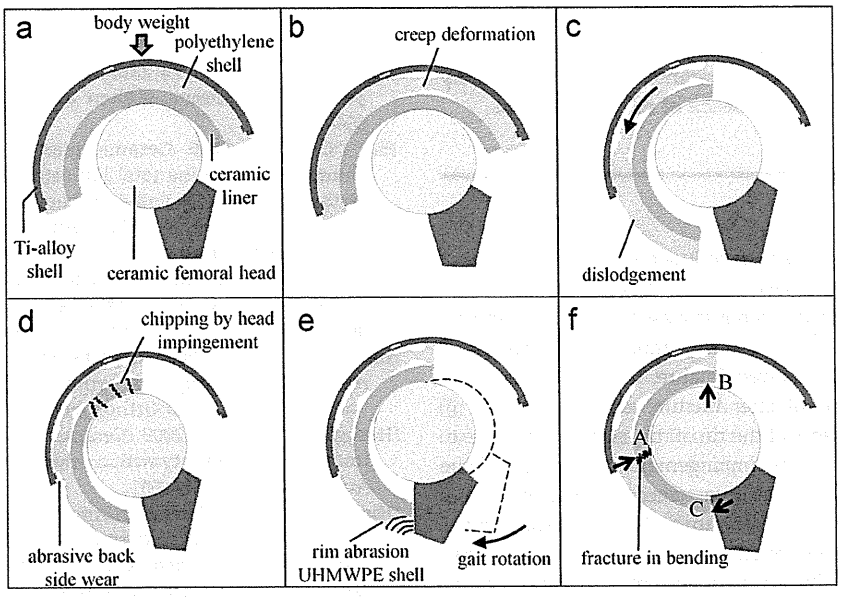

Fig. 7 – Drafts describing the sequence of degradative events that led to the observed liner fracture patterns: (a) sandwich-type hip joint correctly implanted; (b) creep deformation in a limited interval of radial angles of the UHMWPE shell due to body weight; (c) occurrence of dislodgment upon rotation of UHMWPE shell/ceramic liner inside the metal shell; (d) impingement of femoral head on the upper rim of the ceramic liner (i.e., in a state of subluxation) producing chipping of the ceramic liner; (e) impingement of the stem neck on the lower rim of the (rotated) UHMWPE shell, which in turn produced severe abrasions to the shell rim and (f) polar loading (at location A) producing bending of the curved cup component constrained by the supporting points B and C.

(Fig. 7(c)), and such an incorrect implant configuration exacerbated impingements of both femoral head on the upper rim of the ceramic liner (i.e., in a state of subluxation) and stem neck on the lower rim of the UHMWPE shell (cf. Fig. 7(d) and (e)). In addition, Fig. 7(f) schematically shows the state of localized loading on the (rotated) pole of the ceramic cup (integer to the UHMWPE shell). The loading configuration indeed foresees polar loading (at location A in Fig. 7(f)) with bending of the curved cup component upon loading reactions at the supporting points B and C in Fig. 7(f), which corresponded to the rim impingement locations of the femoral head and of the stem neck, respectively. Such loading configuration ultimately led to a single circumferential crack starting from the pole of the ceramic liner and propagating toward the cup base. Experimental evidence supporting the occurrence of such fracture mechanism was searched for on the circumferential fracture surface of the ceramic liner. As shown in Fig. 8, the fracture origin could be found in correspondence of the external surface of the ceramic liner nearby the location where polar pressure was exerted by the metallic shell (location A in Fig. 7(f)).

The complex sequence of mechanisms shown in Fig. 7 can rationally explain the phenomenological observation made on all the analyzed retrievals, with the exception of Case IV. As a matter of fact, the occurrence of multiple crack paths, the observation of no dislodgment in the radiographic preoperative exam, and the lack of any abrasive damage in the UHMWPE shell clearly reveal the occurrence of a different failure mechanism. The ceramic liner was indeed backed by the thinnest among the UHMWPE shells employed by the maker and the fracture pattern suggests a compressive

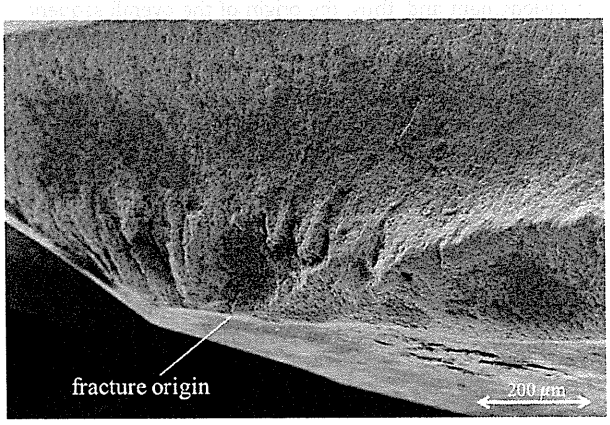

Fig. 8 – Scanning electron micrograph of the fracture origin found on the external side (convex surface) of the fractured surface of the circumferentially broken ceramic liner referred to as Case VI.

fracture event (Espinosa et al., 1998; Zavattieri and Espinosa, 2001), presumably amplified by shocks of the femoral head against the ceramic cup. Recently, Uribe et al. (2011) have presented a focused modeling study of shock-induced damages in ceramic hip prostheses. In this study, the shock-induced stress was determined numerically using finite element analysis and demonstrated that even a minor microseparation effect in an all-ceramic hip implant could cause a severe shock on the bearing surface when the heels touch the ground. Such shock can be as high as nine times the body weight. Owing to the presence of crack initiation sites on

Please cite this article as: Okita, S., et al., Failure analysis of sandwich-type ceramic-on-ceramic hip joints: A spectroscopic investigation into the role of the polyethylene shell component. Journal of the Mechanical Behavior of Biomedical Materials (2013), http://dx.doi.org/10.1016/j.jmbbm.2013.01.022

the bearing surface (i.e., as a consequence of wear scars), one could conclude that the thickness of the ceramic liner could have resulted to be too thin to guarantee structural integrity under gait conditions in the presence of microseparation.

4. Conclusion

In conclusion, a series of six (failed) sandwich implants with *in vivo* lifetimes ranging between 2 and 9 yr (average followup of 6 yr 9 months) was studied in order to classify their mechanisms of failure and the related causes. Among the investigated implants, four implants showed fracture of the ceramic liner. Three different patterns of liner fracture could be located: (i) chipping into several pieces of the rim of the ceramic liner due to subluxation accompanied by impingement and shock of the femoral head against the liner (two cases); (ii) fracture of the liner into two hemispheres by a single circumferential crack path spanning over the entire cup (two cases, of which one also included the pattern in (i)); and (iii) fragmentation fracture of the ceramic liner into a large number of small pieces (one case). In the case of pattern (iii) (i.e., in only one case), dislodgement of the UHMWPE shell/ceramic liner was not observed in pre-operative radiographic analyses. An analysis of the failure events showed that, with the exception of the fracture pattern (iii), all the other ceramic fracture cases were a consequence of dislodgment or of implantation errors. In particular, creep of the polyethylene shell was found to be the triggering phenomenon for dislodgment and, thus, the origin of the overall sequence of failure events. We conclude that failure cases of sandwich-type implants should be classified as design failures rather than ceramic-on-ceramic fractures since no material could stand in its bearing functions when loaded in the incorrect geometry that arose from such a malfunctioning implant mechanics.

Appendix A. Supporting information

Supplementary data associated with this article can be found in the online version at http://dx.doi.org/10.1016/j.jmbbm.2013.01.022.

REFERENCES

Amino, H., 2002. Ceramic on ceramic total hip arthroplasty in Japan. Pharma Medica 20, 19–25 (in Japanese).

Bewill, SL., et al., 2005. Finite element simulation of early creep and wear in total hip arthroplasty. Journal of Biomechanics 38, 2365–2374.

Cameron, H.U., 1991. Ceramic head implantation failures. Journal of Arthroplasty 6, 185–188.

Coventry, M.B., 1985. Late dislocations in patients with Charnley total hip arthroplasty. Journal of Bone and Joint Surgery (American) 67, 832–841.

Dalla Pria, P., et al., 2010. Breakage and noises in ceramic on ceramic couplings. European Journal of Orthopaedic Traumatology 1, 53–59.

Espinosa, H.D., et al., 1998. A finite deformation continuum/discrete model for the description of fragmentation and damage in brittle materials. Journal of the Mechanics and Physics of Solids 46, 1909–1942.

Glyn-Jones, S., 2008. The creep and wear of highly cross-linked polyethylene. Journal of Bone and Joint Surgery (British) 90B, 556–561.

Ha, Y.C., et al., 2006. Ceramic liner fracture after cementless alumina-on-alumina total hip arthroplasty. Clinical Orthopaedics and Related Research 458, 106–110.

Hamadouche, M., et al., 2002. Alumina-on-alumina total hip arthroplasty: a minimum 18.5-year follow-up study. Journal of Bone and Joint Surgery: American 84, 69–77.

Hannouche, D., et al., 2003. Fractures of ceramic bearings: history and present status. Clinical Othopaedics 417, 19–26.

Hasegawa, M., et al., 2006. Cobalt–chromium head wear following revision hip arthroplasty performed after ceramic fracture —a case report. Acta Orthopaedica 77, 833–835.

Hasegawa, M., et al., 2003. Ceramic acetabular liner fracture in total hip arthroplasty with a ceramic sandwich cup. Journal of Arthroplasty 18, 658–661.

Hiss, R., et al., 1999. Hobeika S, Lynn C, Strobl G. Network stretching, slip processes, and fragmentation of crystallites during uniaxial drawing of polyethylene and related copolymers. A comparative study. Macromolecules 32, 4390–4403.

Huo, M.H., et al., 1996. Total hip replacements using the ceramic Mittelmeier prosthesis. Clinical Orthopaedics 332, 143–150.

Kaku, N., et al., 2001. Qualitative analysis of polyethylene wear in a bipolar femoral prosthesis: a case report. Journal of Orthopaedics Surgery 9, 71–76.

Kircher, J., et al., 2009. Extremely high fracture rate of a modular acetabular component with a sandwich polyethylene ceramic insertion for THA: a preliminary report. Archives of Orthopaedic and Trauma Surgery 129, 1145–1150.

Kitajima, S., Hotokebuchi, T., 2003. Ceramic on ceramic total hip arthroplasty. Journal of Joint Surgery 22, 85–89 (in Japanese).

Krikler, S.J., 1997. Fracture of a ceramic femoral head after a revision operation. A case report. Journal of Bone and Joint Surgery: American 79A, 118–121.

Kumakura, T., et al., 2009. In-depth oxidation and strain profiles in UHMWPE acetabular cups non-destructively studied by confocal Raman microprobe spectroscopy. Journal of Biomaterials Science: Polymer Edition 20, 1809–1822.

Kyomoto, M., et al., 2007. Strain in UHMWPE for orthopaedic use studied by Raman microprobe spectroscopy. Journal of Biomaterials Science: Polymer Edition 18, 165–178.

Lewinnek, G.E., et al., 1978. Dislocations after total hip-replacement arthroplasties. Journal of Bone and Joint Surgery: American 60, 217–220.

Maccauro, G., Piconi, C., 2000. Ceramic femoral head fracture in total hip replacement. International Orthopaedics 24, 239.

McCollum, D.E., Gray, W.J., 1990. Dislocation after total hip arthroplasty: causes and prevention. Clinical Orthopaedics and Related Research 261, 159–170.

McLean, C.R., et al., 2002. Delayed fracture of the ceramic femoral head after trauma. Journal of Arthroplasty 17, 503–504.

Messieh, M., et al., 1994. Wear debris from bipolar femoral neck-cup impingement: a cause of femoral stem loosening. Journal of Arthroplasty 9, 89–93.

Oonishi, H., 1992. New design feature of high-quality alumina-alumina ceramic combination in total hip replacement. Bioceramics 5, 403–408.

Park, Y.S., et al., 2006. Ceramic failure after total hip arthroplasty with an alumina-on-alumina bearing. Journal of Bone and Joint Surgery: American 88, 780–787.

Peiro, A., 1991. Fracture of the ceramic head in total hip arthroplasty: report of two cases. Journal of Arthroplasty 6, 371–374.

Pezzotti, G., et al., 2011. Non-destructively differentiating the roles of creep, wear and oxidation in long-term in vivo

Please cite this article as: Okita, S., et al., Failure analysis of sandwich-type ceramic-on-ceramic hip joints: A spectroscopic investigation into the role of the polyethylene shell component. Journal of the Mechanical Behavior of Biomedical Materials (2013), http://dx.doi.org/10.1016/j.jmbbm.2013.01.022

exposed polyethylene cups. Journal of Biomaterials Science: Polymer Edition 22, 2165–2184.

Piconi, C., et al., 1999. Analysis of a failed alumina THR ball head. Biomaterials 20, 1637–1646.

Pulliam, I.T., Trousdale, R.T., 1997. Fracture of a ceramic femoral head after a revision operation. A case report. Journal of Bone and Joint Surgery: American 79, 118–121.

Rudas, M., et al., 2005. Failure of curved brittle layer systems from radial cracking in concentrated surface loading. Journal of Materials Research 20, 2812–2819.

Sariali, E., et al., 2009. Undetected fracture of an alumina ceramic on ceramic hip prosthesis. Journal of Arthroplasty 25 (4), 658.e1–658.e5.

Sedel, L., 2000. Evolution of alumina-on-alumina implants: a review. Clinical Orthopaedics and Related Research 379, 48–54.

Suzuki, K., 2003. Fracture of a ceramic acetabular insert after ceramic-on-ceramic THA—a case report. Acta Orthopaedica Scandinavica 74, 101–103.

Tashiro, K., et al., 1988. Morphological effect on the Raman frequency shift induced by tensile stress applied to crystalline polyoxymethylene and polyethylene: spectroscopic support for the idea of an inhomogeneous stress distribution in polymer material. Polymer 29, 1768–1783.

Tateiwa, T., et al., 2008. Ceramic total hip arthroplasty in the United States: safety and risk issues revisited. American Journal of Orthopedics 37, E26–E31.

Uribe, J., et al., 2011. Finite element modeling of shock-induced damages on ceramic hip prostheses. International Scholarly Research Network, Materials Science Article ID 121486, 1–14.

Widmer, K.H., Zurfluh, B., 2004. Compliant positioning of total hip components for optimal range of motion. Journal of Orthopaedic Research 22, 815–821.

Willmann, G., 2001. Retrieved ceramic wear couple: unexpected findings. In: Toni, A., Willmann, G. (Eds.), Bioceramics in Joint Arthroplasty: Proceedings of the 6th BIOLOX®Symposium. Georg Thieme Verlag, Stuttgart, Germany, pp. 63–65.

Wong, W.F., Young, R.J., 1994. Molecular deformation processes in gel-spun polyethylene fibres using Raman spectroscopy. Journal of Materials Science 29, 510–519.

Woo, R.Y., Morrey, B.F., 1982. Dislocations after total hip arthroplasty. Journal of Bone and Joint Surgery: American 64, 1295–1306.

Yamaguchi, M., et al., 2000. The spatial location of impingement in total hip arthroplasty. Journal of Arthroplasty 15, 305–313.

Yamamoto, K., et al., 2004. Failure of ceramic THR with liner dislocation—a case report. Acta Orthopaedica Scandinavica 75, 500–502.

Zavattieri, P.D., Espinosa, H.D., 2001. Grain level analysis of crack initiation and propagation in brittle materials. Acta Materialia 49, 4291–4311.

Please cite this article as: Okita, S., et al., Failure analysis of sandwich-type ceramic-on-ceramic hip joints: A spectroscopic investigation into the role of the polyethylene shell component. Journal of the Mechanical Behavior of Biomedical Materials (2013), http://dx.doi.org/10.1016/j.jmbbm.2013.01.022

Journals of Gerontology: MEDICAL SCIENCES
Cite journal as: J Gerontol A Biol Sci Med Sci
doi:10.1093/gerona/gls253

Spinal Posture in the Sagittal Plane Is Associated With Future Dependence in Activities of Daily Living: A Community-Based Cohort Study of Older Adults in Japan

Kojiro Kamitani,[1,2] Takehiro Michikawa,[3] Satoko Iwasawa,[4] Norihito Eto,[5] Taichiro Tanaka,[1] Toru Takebayashi,[4] and Yuji Nishiwaki[1]

[1]Department of Environmental and Occupational Health, School of Medicine, Toho University, Tokyo, Japan.
[2]Department of Orthopedics, Ota General Hospital, Kanagawa, Japan.
[3]Environmental Epidemiology Section, Center for Environmental Health Sciences, National Institute for Environmental Studies, Tsukuba, Japan.
[4]Department of Preventive Medicine and Public Health, School of Medicine, Keio University, Tokyo, Japan.
[5]Department of Biomedical Engineering, School of Engineering, Tokai University, Kanagawa, Japan.

Address correspondence to Yuji Nishiwaki, MD, MSc, PhD, Department of Environmental and Occupational Health, School of Medicine, Toho University, 5-21-16 Omori-nishi, Otaku, Tokyo 143-8540, Japan. E-mail: yuuji.nishiwaki@med.toho-u.ac.jp

Background. Accumulated evidence shows how important spinal posture is for aged populations in maintaining independence in everyday life. However, the cross-sectional designs of most previous studies prevent elucidation of the relationship between spinal posture and future dependence in activities of daily living (ADL). We tried to clarify the association by measuring spinal posture noninvasively in a community-based prospective cohort study of older adults, paying particular attention to thoracic curvature, lumbar curvature, sacral hip angle, and inclination to determine which parameter is most strongly associated with dependence in ADL.

Methods. Spinal posture was evaluated in 804 participants (338 men, 466 women, age range: 65–94 years) who were independent in ADL at baseline. We defined dependence in ADL as admission to a nursing home or need of home assistance. During the 4.5-year follow-up period, 126 (15.7%) participants became dependent in ADL. The relationship between the spinal posture parameters and outcome was assessed by dividing the participants into sex-specific quartiles of the parameters.

Results. Only inclination (angle subtended between the vertical and a line joining C7 to the sacrum) was associated with outcome, although lumbar curvature also showed a marginal association. The age- and sex-adjusted odds ratio for a 1 unit increase in the quartiles of inclination was 1.79 (confidence interval: 1.44, 2.23). After mutual adjustment for the 4 parameters, statistical significance for inclination still remained, with no substantial changes in the association estimates.

Conclusions. This study indicates that spinal inclination is associated with future dependence in ADL among older adults.

Received July 12, 2012; Accepted November 14, 2012

Decision Editor: Stephen Kritchevsky, PhD

POPULATIONS are aging rapidly worldwide. This trend is particularly evident in Japan, whose population has the world's longest life expectancy (79.4 years for men and 85.9 years for women (1)). The already rapid pace at which society is aging is expected to accelerate further, meaning that fewer young people will be available to take care of the elderly people, and thus making it even more important for the elderly people to be able to live independent and active lives.

Spinal posture changes with age, but accumulated evidence shows that continued good spinal posture is important in allowing the aged to maintain independent lives (2,3). Hirose and colleagues (4) reported that the posture of the trunk in the sagittal plane is associated not only with the distance and time parameters of gait, but also with functional performance in the elderly population. In a study by Takahashi and colleagues (5), participant groups with trunk deformities tended to score lower than the control group on subjective healthiness and life satisfaction measures. However, the cross-sectional designs of most studies to date prevent conclusions being drawn about the relationship between spinal posture and future dependence in activities of daily living (ADL). The participants of these studies were patients with spinal deformities and diagnoses of osteoporosis, and evidence is lacking from community-based studies.

Determination of spinal posture requires the examination of multiple elements, including the cervical vertebrae, thoracic vertebrae, lumbar vertebrae, and pelvis. Because such examinations have generally been done with x-ray equipment, they have not been carried out at local health facilities due to the lack of specialized equipment. In recent years, however, a computer-assisted and easily operated, noninvasive, portable device to measure spinal shape has been developed (6,7). With this device, sagittal spinal curve divided into thoracic curvature, lumbar curvature, sacral hip angle, and inclination can be examined. We used the device in this study to examine spinal posture noninvasively in older adults and tried to clarify the association between spinal posture and future dependence in ADL through a community-based prospective cohort study design. We paid particular attention to thoracic curvature, lumbar curvature, sacral hip angle, and inclination to determine which of these four parameters is most strongly associated with dependence in ADL.

Methods

Study Population

The Kurabuchi Study, a community-based prospective cohort study of aging involving functional assessment of an older population, was launched in 2005 (8,9). Briefly, the study population included all residents aged 65 years or older of Kurabuchi Town, Gunma Prefecture (approximately 100 km north of Tokyo, Japan). Excluding those who were hospitalized or institutionalized, a total of 1,294 residents, were eligible for inclusion in the study. Of these, 834 participated in the baseline examination (participant proportion = 64.5%) and gave written informed consent. For the purposes of this study, we excluded those who were dependent in ADL at the baseline (n = 29) and those who did not undergo spinal curvature measurements (n = 1). Thus, a total of 804 participants (338 men and 466 women) were subject to the study. The study protocol was approved by the Ethics Committee of the School of Medicine, Keio University (Tokyo, Japan) and by that of Toho University (Tokyo, Japan).

Assessment of Spinal Posture

The participants were asked to stand in a relaxed position wearing one layer of clothing, and spinal posture was evaluated with a Spinal Mouse (Indiag, Volkerswill, Switzerland), a computer-assisted, noninvasive device for measuring spinal shape. The device is guided along the midline of the spine, starting at the spinous process at C7 and finishing at the top of the anal crease (approximately S3). Measurements were repeated 3 times, and the best two values were averaged. The relevant parameters recorded with the Spinal Mouse were thoracic curvature (Th1-2 to Th11-12), lumbar curvature (Th12–L1 to the sacrum), sacral hip angle (angle between a straight line from S1 to S3 and true vertical), and trunk angle of inclination (angle between a straight line from Th1 to S1 and true vertical (6)), as shown Figure 1. The larger the figures for thoracic and lumbar curvature measurements were, the greater the degree of kyphosis. The sacral hip angle and inclination measurements reflected forward pelvic tilt and forward stooped posture.

The intraexaminer reliability and interexaminer reliability of the Spinal Mouse were high in terms of intraclass correlation coefficients: 0.82–0.95 (6,7) and 0.81–0.86 (7), respectively.

Outcome Measurements

We defined dependence in ADL as either admission to a nursing home or need of assistance at home during the follow-up period (10). The latter was defined as long-term care (LTC) eligibility or a need for help in any of the six basic ADL items in the Katz Index of independence in ADL (11). LTC eligibility is a requirement for receiving LTC insurance services in Japan, which began in 2000. In this study, any of the seven levels of LTC insurance services was considered LTC eligible. Information on death, nursing home admission, and LTC eligibility was obtained from the Kurabuchi Branch Office of Takasaki City Hall. Information on Katz ADL was obtained from repeat face-to-face home interviews conducted every year until 2010 by public health nurses and local welfare commissioners, and occurrence of ADL dependence in any year was defined as dependence in ADL.

Covariates

We collected information on age, sex, smoking status (current vs former or never), alcohol drinking (current vs

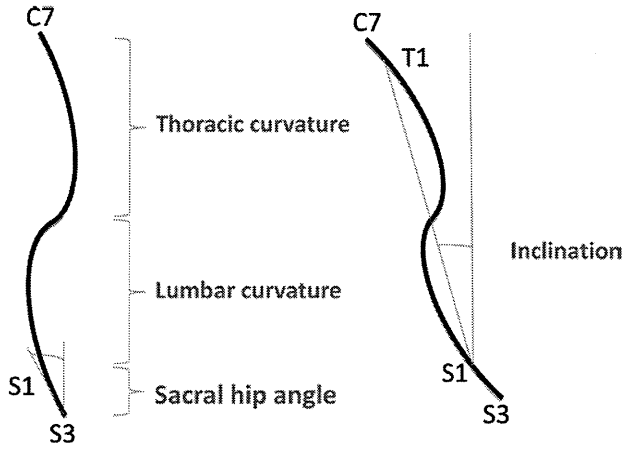

Figure 1. A schema illustrating the four parameters. Thoracic curvature: thoracic kyphosis (corresponds to Cobb angle between Th1 and Th12). Lumbar curvature: lumbar kyphosis (corresponds to Cobb angle between Th12 and S1). Sacral hip angle: the angle between a straight line from S1 to S3 and true vertical. Inclination: the angle between a straight line from Th1 to S1 and true vertical.

former or never), educational level (junior high vs high school or higher), back pain, including low back pain (yes or no in the past year), knee joint pain (never vs occasionally vs often vs always), and current or past history of life-threatening diseases, including stroke, myocardial infarction/angina, diabetes mellitus, and cancer (summary answer of yes or no). Body mass index was calculated as weight (kg) divided by the square of height (m) predicted by demi-span (12) and then categorized (<18.5 vs 18.5–24.9 vs 25≤ kg/m^2). Estimated bone mineral density was assessed from calcaneal quantitative ultrasound measurements made with an A-1000 Express (GE Yokogawa Medical Systems, Tokyo, Japan) and expressed as a stiffness index. All of the above covariates have been reported to be involved in ADL dependence outcomes.

Statistical Analysis

All analyses were performed with STATA version 12 (STATA Corporation, College Station, Texas).

Distributions of the four parameters of spinal posture were calculated according to age and sex. Trends by age category were examined with logistic regression, with consecutive integers given to each category. The relationships between the spinal posture parameters and outcomes were assessed by dividing the participants into sex-specific quartiles. First, age-category (5-year increments) and sex-adjusted analyses were carried out with logistic regression models. Then, other covariates (education, current/past history of life-threatening diseases, knee joint pain, and body mass index category) were included in the models (Model 1). Smoking and drinking status were not included because they were not associated with outcomes in this study. Second, a model mutually adjusted for all four parameters of spinal posture (Model 2) was applied. Additionally, models including back pain and stiffness were applied to Model 2 (Model 3). Trends across increasing quartiles of the parameters were also calculated by treating the quartiles as an integral value. Because there was no interaction by sex, all analyses were carried out with combined data for men and women. This analytic method was repeated for dependence in ADL and for the composite outcome of dependence in ADL and death. Participants who died during the follow-up period were excluded from the analysis of dependence in ADL. Odds ratios (ORs) and 95% confidence intervals (95% CIs) were used to describe the strengths of associations.

Results

During the 4.5-year follow-up period, 126 (16.4%) participants became dependent in ADL, 61 (7.6%) died, and 6 (0.7%) moved out of the town. Table 1 shows the characteristics of the study participants. Those in their seventies constituted the majority and women made up to 58%. The distributions of the four parameters of spinal posture

Table 1. Characteristics of the Study Participants (n = 804; Kurabuchi Study 2005)

		n (%)*
Age category (y)	65–69	174 (21.7)
	70–74	237 (29.5)
	75–79	193 (24.0)
	80–84	137 (17.0)
	85	63 (7.8)
Sex	Men	338 (42.0)
	Women	466 (58.0)
Current smoking	Yes	101 (12.9)
	No	680 (87.1)
Current drinking	Yes	245 (31.6)
	No	530 (68.4)
Education	High school or higher	182 (23.5)
	Junior high school or below	593 (76.5)
History of life-threatening diseases†	Yes	189 (24.5)
	No	582 (75.5)
Back pain	Yes	480 (59.7)
	No	324 (40.3)
Knee joint pain	Never	419 (54.1)
	Occasionally	170 (22.0)
	Often	63 (8.1)
	Always	122 (15.8)
BMI category (kg/m^2)‡	<18.5	87 (10.8)
	18.5–24.9	511 (63.6)
	≥25	205 (25.5)
Stiffness	Mean (*SD*)	71.4 (16.8)

Notes: SD = standard deviation; BMI = body mass index.

*Due to missing values, the totals for the stratified subgroups are not equal.

†Stroke, myocardial infarction or angina, diabetes mellitus, and cancer were included.

‡BMI was calculated as weight (kg) divided by the square of height (m) predicted by demi-span (12).

are presented in Table 2. The effect of age on thoracic curvature seemed to vary between men and women. In men, thoracic kyphosis decreased with age, whereas it appeared to increase with age in women. However, the trend was not statistically significant. Lumbar lordosis decreased and inclination increased with age in both men and women.

The associations of the four parameters of spinal posture with future dependence in ADL are summarized in Table 3. In Model 1, only inclination was associated with outcome, although lumbar curvature and sacral hip angle showed marginal associations. When the lowest quartile of inclination was used as a reference, the adjusted ORs (95% CI) for the second, third, and highest quartiles were 1.46 (0.60, 3.59), 3.90 (1.76, 8.63), and 4.93 (2.23, 10.91), respectively. The adjusted OR for a 1 unit increase in the quartiles of inclination was 1.75 (1.39, 2.20). Even when inclination was included in the model as a continuous variable, the adjusted OR for a 1 unit increase in inclination was 1.04 (1.02–1.06). In the model where the four parameters were mutually adjusted (Model 2), statistical significance for inclination was maintained, and the association estimates did not change substantially. When back pain and stiffness were added as covariates, the ORs were essentially the same as those in

Table 2. Distributions of the parameters of spinal curvature by age and sex

Age category (y)	*n*	Thoracic curvature Median (25, 75 percentiles)	Lumbar curvature Median (25, 75 percentiles)	Sacral hip angle Median (25, 75 percentiles)	Inclination Median (25, 75 percentiles)
Men & Women ($n = 804$)					
65–69	174	44 (37, 50)	–13.5 (–22, –4)	7 (1, 13)	7 (5, 11)
70–74	237	41 (32, 49)	–10 (–18, 0)	7 (0, 12)	9 (6, 11)
75–79	193	43 (35, 50)	–5 (–15, 6)	6 (0, 12)	12 (8, 17)
80–84	137	40 (30, 49)	0 (–11, 10)	4 (–2, 12)	13 (9, 22)
85–	63	44 (30, 54)	–2 (–14, 15)	5 (–1, 14)	16 (10, 29)
trend*		$p = 0.234$	$p < 0.001$	$p = 0.083$	$p < 0.001$
Men ($n = 338$)					
65–69	74	47.5 (40, 54)	–14.5 (–24, –4)	4.5 (1, 14)	8 (6, 12)
70–74	103	41 (31, 49)	–10 (–17, –1)	6 (0, 13)	9 (7, 12)
75–79	82	43.5 (36, 49)	–8 (–17.5, 3)	7 (0, 12)	12 (7, 16)
80–84	54	40 (29, 48)	0 (–9, 9)	3.5 (–2, 12)	11 (8, 20)
85–	25	39 (29, 51)	–2 (–14, 17)	4 (1, 12)	10 (9, 21)
trend*		$p < 0.001$	$p < 0.001$	$p = 0.172$	$p < 0.001$
Women ($n = 466$)					
65–69	100	41 (35, 48.5)	–13 (–21.5, –3.5)	8.5 (3, 12.5)	7 (4, 11)
70–74	134	41 (32, 50)	–10 (–18, 3)	7 (0, 11)	9 (6, 13)
75–79	111	43 (32, 50)	–4 (–14, 8)	5 (0, 13)	12 (9, 18)
80–84	83	42 (34, 51)	1 (–14, 12)	4 (–1, 13)	14 (9, 23)
85–	38	45 (33, 58)	–2.5 (–16, 14)	5.5 (1, 14)	17 (13, 29)
trend*		$p = 0.173$	$p < 0.001$	$p = 0.277$	$p < 0.001$

*Trend was examined by scoring the age category (1 to 5) as a continuous term in the regression analysis.

Table 3. Associations of the parameters with dependence in activities of daily living

		Median (25, 75 percentiles)	n/N (%)	Age- & sex-adjusted OR (95% CI)	Adjusted OR (95% CI) Model 1*	Adjusted OR (95% CI) Model 2**	Adjusted OR (95% CI) Model 3***
Thoracic curvature	Q1	27 (22, 30)	29/168 (17.3)	1.00	1.00	1.00	1.00
	Q2	38 (36, 40)	38/183 (20.8)	1.73 (0.96–3.10)	1.81 (0.98–3.34)	2.04 (1.05–3.96)	2.05 (1.05–4.00)
	Q3	45 (44, 48)	30/188 (16.0)	1.17 (0.64–2.14)	1.17 (0.62–2.20)	1.37 (0.68–2.76)	1.42 (0.70–2.85)
	Q4	56 (52, 61)	29/198 (14.7)	0.94 (0.51–1.71)	0.75 (0.39–1.44)	0.92 (0.43–1.96)	0.89 (0.41–1.92)
	one unit increase in the quartiles			0.94 (0.79–1.13)	0.89 (0.73–1.08)	0.98 (0.77–1.23)	0.97 (0.77–1.23)
Lumbar curvature	Q1	−24 (−28, −20)	20/188 (10.6)	1.00	1.00	1.00	1.00
	Q2	−12 (−15, −10)	24/194 (12.4)	1.07 (0.55–2.08)	1.20 (0.60–2.42)	1.07 (0.47–2.44)	1.08 (0.47–2.46)
	Q3	−2 (−4, 0)	39/186 (21.0)	1.77 (0.95–3.30)	1.72 (0.89–3.33)	1.50 (0.57–3.98)	1.47 (0.55–3.93)
	Q4	13 (8, 28)	43/169 (25.4)	1.65 (0.88–3.07)	1.71 (0.88–3.33)	1.52 (0.47–4.92)	1.38 (0.42–4.50)
	one unit increase in the quartiles			1.22 (1.00–1.48)	1.21 (0.99–1.48)	1.20 (0.81–1.76)	1.17 (0.79–1.72)
Sacral hip angle	Q1	−5 (−9, −2)	28/165 (17.0)	1.00	1.00	1.00	1.00
	Q2	3 (1, 4)	32/189 (16.9)	1.10 (0.61–2.00)	1.20 (0.65–2.24)	1.27 (0.62–2.61)	1.28 (0.62–2.62)
	Q3	9 (7, 11)	27/198 (13.6)	1.14 (0.61–2.11)	1.17 (0.60–2.26)	1.32 (0.56–3.14)	1.22 (0.51–2.93)
	Q4	16 (15, 20)	39/185 (21.1)	1.63 (0.91–2.92)	1.83 (0.98–3.42)	2.26 (0.87–5.85)	2.20 (0.84–5.73)
	one unit increase in the quartiles			1.17 (0.97–1.41)	1.20 (0.98–1.47)	1.30 (0.95–1.78)	1.29 (0.94–1.77)
Inclination	Q1	4 (3, 6)	10/185 (5.4)	1.00	1.00	1.00	1.00
	Q2	8 (7, 9)	15/180 (8.3)	1.48 (0.63–3.48)	1.46 (0.60–3.59)	1.34 (0.54–3.33)	1.43 (0.57–3.57)
	Q3	12 (11, 13)	42/199 (21.1)	3.71 (1.75–7.85)	3.90 (1.76–8.63)	3.32 (1.43–7.69)	3.28 (1.41–7.62)
	Q4	20 (16, 27)	59/173 (34.1)	5.30 (2.51–11.18)	4.93 (2.23–10.91)	3.65 (1.43–9.37)	3.47 (1.35–8.93)
	one unit increase in the quartiles			1.79 (1.44–2.23)	1.75 (1.39–2.20)	1.67 (1.25–2.23)	1.62 (1.21–2.17)

Notes: OR: odds ratio, CI: confidence interval.
In this analysis, residents who died during the follow-up period (n = 61) were excluded.
*Age category, sex, educational category, history of life-threatening diseases (stroke, myocardial infarction/angina, diabetes mellitus, and cancer), knee joint pain and body mass index category were adjusted for.
**In addition to the variables included in Model 1, all parameters (thoracic curvature, lumbar curvature, sacral hip angle, inclination) were mutually adjusted.
***Back pain and stiffness were added to Model 2.

Model 2. When the analysis was repeated for the composite outcome of dependence in ADL and death, the association of inclination with outcome was only slightly attenuated and remained statistically significant. The adjusted ORs for 1 unit increases in the quartiles of inclination were 1.52 (1.19, 1.93) in Model 2 and 1.50 (1.18, 1.91) in Model 3 for the composite outcome of dependence in ADL and death.

Discussion

We evaluated four parameters of spinal posture (thoracic curvature, lumbar curvature, sacral hip angle, and inclination) in older adults and demonstrated for the first time, after 4.5 years of follow-up, that of the four parameters, inclination has the greatest effect on dependence in ADL with no clear threshold. We showed too that this association was independent of back pain and estimated bone mineral density. Our results indicate that attention needs to be paid to inclination in spinal posture to identify elderly people at high risk of becoming dependent in ADL.

Many reports have indicated that posture of the trunk in the sagittal plane is associated with body function and dependence in ADL. Various methods of measuring spinal posture were used in these studies. Leech and colleagues (13) and Lombardi and colleagues (14) measured the Cobb angle to assess kyphosis, and reported that hyperkyphosis might be associated with pulmonary function. In another study, participants lay supine with the neck in a neutral position and occiput to table distance was measured with 1.7-cm blocks placed between the head and the examination table; moderate hyperkyphotic posture was found to indicate an increased risk of injurious falls in older men, with a less pronounced association in older women (15). Ryan and colleagues (16) evaluated kyphosis through measurement of the distance between the occiput and a wall, finding that kyphosis is associated with ADL decline. Takahashi and colleagues (5) examined sagittal spinal posture using lateral-view photographs of the participants and found that groups with trunk deformities tended to score lower than the control group on subjective measures of healthiness and life satisfaction. The abovementioned methods of kyphosis assessment are easy and useful, requiring no medical information from local health centers. However, they evaluate spinal posture as a whole, making assessment of each composite parameter of spinal posture impossible. We overcame this disadvantage by using a noninvasive device for measuring spinal shape that has been developed in recent years, the Spinal Mouse.

In our study, mutual adjustment for the four parameters of spinal posture showed that only inclination is associated with future dependence in ADL. Other cross-sectional studies using the Spinal Mouse may help explain this association. Sakamitsu and colleagues (17) used the Spinal Mouse to measure balance (1 ft standing with eyes open) and gait (walking speed in 10-m walk and walking distance in 3 min) in 28 elderly people. They concluded that the larger the anterior inclination of the trunk, the greater the decline in balance and gait skills was. A study by Ishikawa and colleagues (18) of 93 osteoporotic patients with a mean age of 70 years showed that forward spinal inclination with a forward stooped posture affected postural balance. It is reasonable to suppose, therefore, that declines in balance and gait skills caused by inclination lead to falls and fractures, and that these negative outcomes in turn lead to dependence in ADL among elderly people. In fact, data exist to show that community-dwelling women with osteoporosis and hyperkyphosis have weaker back extensor strength, weaker lower extremity strength, slower gait, poorer balance, and greater body sway, which as a result gives them a propensity to fall (19).

The line of gravity line moves naturally with changes in spinal alignment (20–22). Arita and colleagues (23) reported that the center of gravity runs anterior to L4-5 and 6 mm anterior to the hip joint in most elderly people, and another study showed that the center of gravity runs anterior to L4 in healthy elderly people (24). The gravity line moves further anterior as inclination of the trunk increases.

In one study, full-length, free-standing radiographs of the spine and pelvis were examined in 125 adult patients with spinal deformities. The study demonstrated that the T1 spinopelvic inclination (the angle between the T1-hip axis and vertical) correlated with Health-Related Quality of Life measures (25). In another study, 752 patients with spinal deformities were enrolled from a multicenter prospective database. Positive sagittal balance was defined as an anterior deviation of the plumb line from the seventh cervical spinous process. This study showed that although even mildly positive sagittal balance is somewhat detrimental, the decline in health status increases in a linear fashion with progressive sagittal imbalance (26).

Some reports in Japanese indicated that lumbar lordosis decreased with increase in age (27,28) and our results supported these earlier studies. Lumbar lordosis is also reported to be associated with decline in walking ability and in muscle power of lower limb (28–30). In this study, however, lumbar curvature only showed a marginal association with future dependence in ADL. If we included inclination in the model, this association disappeared. Whereas, thoracic kyphosis decreased with age among men. Among women, on the contrary, thoracic kyphosis tended to increase with age as reported in other studies (2,29,31). Although we could not explain this sex difference, thoracic kyphosis might decrease as a compensation for the decrease in lumbar lordosis in men. These potential difference between Japanese and people in other countries and between men and women needs further study.

Although we examined only spinal posture in this study, we recognize that examination of lower limb alignment is also important because changes in spinal posture can influence the alignment of the legs: burdens requiring more than the normal compensatory reactions can lead to joint diseases such as osteoarthritis, which in turn lead to declines in

ADL. Such being the case, future studies including evaluations of lower limb alignment are necessary. Although the Spinal Mouse method was easy and useful for evaluating sagittal spinal posture as a whole, it does not seem to be a reliable tool yet for measuring intersegmental spinal range of motion (7). Furthermore, the Spinal Mouse method does not measure spinopelvic alignment. When sagittal unbalance is detected with Spinal Mouse method, therefore, we recommend full x-ray investigation for evaluating spine and pelvis. Another limitation of our study is that we focused only on sagittal spinal posture. Differences in body sizes and lifestyles also mean that caution is necessary in applying our results to other populations. However, we believe our conclusion that inclination is associated with future dependence in ADL among older adults warrants wide attention.

FUNDING

This work was supported by a grant in aid from the Ministry of Health, Labour and Welfare, Japan (H20-Choujyu-009).

ACKNOWLEDGMENTS

The authors would like to thank the staff of the City person & Health Division, Kurabuchi Branch Office, Takasaki City Hall, Gunma prefecture, Japan for their valuable help.

REFERENCES

1. Ministry of Health, Labour and Welfare, Japan. 2011. http://www.mhlw.go.jp/toukei/saikin/hw/life/life11/dl/life11-14.pdf. Accessed July 26, 2012.
2. Nishiwaki Y, Kikuchi Y, Araya K, et al. Association of thoracic kyphosis with subjective poor health, functional activity and blood pressure in the community-dwelling elderly. *Environ Health Prev Med.* 2007;12:246–250.
3. Kado DM, Prenovost K, Crandall C. Narrative review: hyperkyphosis in older persons. *Ann Intern Med.* 2007;147:330–338.
4. Hirose D, Ishida K, Nagano Y, Takahashi T, Yamamoto H. Posture of the trunk in the sagittal plane is associated with gait in community-dwelling elderly population. *Clin Biomech (Bristol, Avon).* 2004;19:57–63.
5. Takahashi T, Ishida K, Hirose D, et al. Trunk deformity is associated with a reduction in outdoor activities of daily living and life satisfaction in community-dwelling older people. *Osteoporos Int.* 2005;16:273–279.
6. Mannion AF, Knecht K, Balaban G, Dvorak J, Grob D. A new skin-surface device for measuring the curvature and global and segmental ranges of motion of the spine: reliability of measurements and comparison with data reviewed from the literature. *Eur Spine J.* 2004;13:122–136.
7. Post RB, Leferink VJ. Spinal mobility: sagittal range of motion measured with the SpinalMouse, a new non-invasive device. *Arch Orthop Trauma Surg.* 2004;124:187–192.
8. Michikawa T, Nishiwaki Y, Kikuchi Y, et al. Gender-specific associations of vision and hearing impairments with adverse health outcomes in older Japanese: a population-based cohort study. *BMC Geriatr.* 2009;9:50.
9. Michikawa T, Nishiwaki Y, Asakura K, et al. Sunlight exposure may be a risk factor of hearing impairment: a community-based study in Japanese older men and women. *J Gerontol A Biol Sci Med Sci.* 2012;68:96–103.
10. Nishiwaki Y, Michikawa T, Yamada M, Eto N, Takebayashi T; Kurabuchi Study Group. Knee pain and future self-reliance in older adults: evidence from a community-based 3-year cohort study in Japan. *J Epidemiol.* 2011;21:184–190.
11. Katz S, Ford AB, Moskowitz RW, Jackson BA, Jaffe MW. Studies of illness in the aged. The index of adl: a standardized measure of biological and psychosocial function. *JAMA.* 1963;185:914–919.
12. Nishiwaki Y, Michikawa T, Eto N, Takebayashi T. Body mass index misclassification due to kyphotic posture in Japanese community-dwelling adults aged 65 years and older. *J Gerontol A Biol Sci Med Sci.* 2011;66:326–331.
13. Leech JA, Dulberg C, Kellie S, Pattee L, Gay J. Relationship of lung function to severity of osteoporosis in women. *Am Rev Respir Dis.* 1990;141:68–71.
14. Lombardi I Jr, Oliveira LM, Mayer AF, Jardim JR, Natour J. Evaluation of pulmonary function and quality of life in women with osteoporosis. *Osteoporos Int.* 2005;16:1247–1253.
15. Kado DM, Huang MH, Nguyen CB, Barrett-Connor E, Greendale GA. Hyperkyphotic posture and risk of injurious falls in older persons: the Rancho Bernardo Study. *J Gerontol A Biol Sci Med Sci.* 2007;62:652–657.
16. Ryan SD, Fried LP. The impact of kyphosis on daily functioning. *J Am Geriatr Soc.* 1997;45:1479–1486.
17. Sakamitsu T, Urabe Y, Yamamoto T. Relationship of kyphosis with balance and walking ability in the elderly. *Rigakuryoho Kagaku.* 2007;22:489–494 (in Japanese with English abstract).
18. Ishikawa Y, Miyakoshi N, Kasukawa Y, Hongo M, Shimada Y. Spinal curvature and postural balance in patients with osteoporosis. *Osteoporos Int.* 2009;20:2049–2053.
19. Sinaki M, Brey RH, Hughes CA, Larson DR, Kaufman KR. Balance disorder and increased risk of falls in osteoporosis and kyphosis: significance of kyphotic posture and muscle strength. *Osteoporos Int.* 2005;16:1004–1010.
20. Thomas DP, Whitney RJ. Postural movements during normal standing in man. *J Anat.* 1959;93:524–539.
21. Asmussen E. The weight-carrying function of the human spine. *Acta Orthop Scand.* 1960;29:276–290.
22. Woodhull AM, Maltrud K, Mello BL. Alignment of the human body in standing. *Eur J Appl Physiol Occup Physiol.* 1985;54:109–115.
23. Arita C, Kobayashi I. The analysis of the posture of the senile. *Rinshouseikeigeka.* 1980;15:115–122 (in Japanese).
24. Harada T, Motegi M, Okazima Y, Hasegawa K, Abe H, Tsuruoka H. Posture of the aged. *Sougouriha.*1994;22:133–136 (in Japanese).
25. Lafage V, Schwab F, Patel A, Hawkinson N, Farcy JP. Pelvic tilt and truncal inclination: two key radiographic parameters in the setting of adults with spinal deformity. *Spine.* 2009;34:E599–E606.
26. Glassman SD, Bridwell K, Dimar JR, Horton W, Berven S, Schwab F. The impact of positive sagittal balance in adult spinal deformity. *Spine.* 2005;30:2024–2029.
27. Hatake K, Nakano T, Ochi T, Inaba D, Yasuoka H. Comparison of spinal alignment in healthy women and old women with vertebral compression fracture –Consideration of compensated spinal alignment. *Therap Res.* 2008;29:597–600 (in Japanese).
28. Miyazaki J, Murata S, Otao H, Horie J, Murata J, Suzuki S. Relationship between physical function and spinal sagittal plane alignment of elderly men. *Rigakuryoho Kagaku.* 2009;24:907–911 (in Japanese with English abstract).
29. Iwaya T, Shirakihara N, Tobimatu Y. The effects of low back pain on physical and social function in elderly people living in rural area. *J Jpn Soc Lumbar Spine Disord.* 2005;11:27–34 (in Japanese).
30. Kai Y, Murata S, Otao H, et al. A relationship between spinal deformity and lower limb muscle strength in community-dwelling elderly females. *Rigakuryoho Kagaku.* 2009;24:45–48 (in Japanese with English abstract).
31. Mori S. Guaging the impact of vertebral compression fractures and spinal deformity on the level of daily activity in patients with osteoporosis. *J Jpn Soc Lumbar Spine Disord.* 2002;8:58–63 (in Japanese with English abstract).

Takiguchi et al. Molecular Pain 2012, 8:31
http://www.molecularpain.com/content/8/1/31

MOLECULAR PAIN

RESEARCH Open Access

Distinct degree of radiculopathy at different levels of peripheral nerve injury

Noboru Takiguchi[1], Munehito Yoshida[1], Wataru Taniguchi[1], Hiroshi Hashizume[1], Hiroshi Yamada[1], Nobuyuki Miyazaki[1], Naoko Nishio[1] and Terumasa Nakatsuka[2*]

Abstract

Background: Lumbar radiculopathy is a common clinical problem, characterized by dorsal root ganglion (DRG) injury and neural hyperactivity causing intense pain. However, the mechanisms involved in DRG injury have not been fully elucidated. Furthermore, little is known about the degree of radiculopathy at the various levels of nerve injury. The purpose of this study is to compare the degree of radiculopathy injury at the DRG and radiculopathy injury proximal or distal to the DRG.

Results: The lumbar radiculopathy rat model was created by ligating the L5 nerve root 2 mm proximal to the DRG or 2 mm distal to the DRG with 6.0 silk. We examined the degree of the radiculopathy using different points of mechanical sensitivity, immunohistochemistry and *in vivo* patch-clamp recordings, 7 days after surgery. The rats injured distal to the DRG were more sensitive than those rats injured proximal to the DRG in the behavioral study. The number of activated microglia in laminas I–II of the L5 segmental level was significantly increased in rats injured distal to the DRG when compared with rats injured proximal to the DRG. The amplitudes and frequencies of EPSC in the rats injured distal to the DRG were higher than those injured proximal to the DRG. The results indicated that there is a different degree of radiculopathy at the distal level of nerve injury.

Conclusions: Our study examined the degree of radiculopathy at different levels of nerve injury. Severe radiculopathy occurred in rats injured distal to the DRG when compared with rats injured proximal to the DRG. This finding helps to correctly diagnose a radiculopathy.

Keywords: Radiculopathy, Microglia, Patch-clamp

Background

There are many patients who suffer from radiculopathy, characterized by spontaneous pain, weakness and numbness in the buttock, leg, and foot and difficulty in controlling specific muscles. Radiculopathy can occur in any part of the spine, most commonly in the lower back (lumbar radiculopathy) and neck (cervical radiculopathy) and not in the middle of the spine (thoracic radiculopathy). Radiculopathy is caused by compression or irritation of the spinal nerves. This can be due to mechanical compression of the nerve by a disc herniation or thickening of surrounding ligaments. Other causes of radiculopathy include diabetes, which can decrease the normal blood flow to the spinal nerves. Inflammation from trauma can also lead to radiculopathy from direct irritation of the nerves.

Radiculopathy is thought to be caused by a series of changes in the sensory processing system, functional reorganization of sensory transmission and development of neural plasticity, in both the peripheral and central nervous systems. Basic research has tended to focus on nerve injury preventing spinal cord neurons from receiving sensory information and relaying it to the brain. The superficial dorsal horn, especially the substantia gelatinosa (SG; lamina horn), plays an important role in modulating nociceptive transmission [1]. In previous studies, whole cell patch-clamp techniques have been adapted to SG neurons in a spinal cord slice with an attached dorsal root to investigate synaptic responses to peripheral nerve stimulation [2,3]. These studies revealed that SG neurons exhibit a variety of excitatory synaptic responses, however it remains

* Correspondence: nakatsuka@kansai.ac.jp
[2]Pain Research Center, Kansai University of Health Sciences, 2-11-1 Wakaba Kumatori Sennan, Osaka 590-0482, Japan
Full list of author information is available at the end of the article

to be settled what kinds of stimulation applied to the skin elicit these responses.

Wind-up is a progressive, frequency-dependent facilitation of neuronal responses induced by repetitive electrical stimulation of afferent C-fibers [4]. Long-term potentiation (LTP) of excitatory synaptic transmission is a long-lasting enhancement in signal transmission between two neurons that results from stimulating them synchronously. It is one of several phenomena underlying synaptic plasticity, the ability of chemical synapses to change their strength. LTP is synaptic plasticity not only in the peripheral nervous system and brain, but also in the spinal cord [5]. The cellular mechanisms of central sensitization and its relationship to the hypersensitivity and hyperalgesia of radiculopathy are still not fully elucidated. Previous research has used *in vivo* patch-clamp techniques to analyze excitatory synaptic responses evoked by cutaneous mechanical stimuli [6,7]. An *in vivo* preparation of a rat spinal cord was used to investigate the superficial dorsal horn neuron response to naturally applied noxious cutaneous stimuli, offering a more comprehensive study of nociceptive processing in the rats superficial dorsal horn.

Nerve injury produces the activation of not only neurons but also glial cells in the central nervous system (CNS) [8-10]. Glial cells make up over 70% of the total cell population in the CNS and are classified into astrocytes, oligodendrocytes, and microglia. Microglia activation following nerve injury is significantly increased compared with oligodendrocytes and astrocytes. Microgliosis (accumulation of activated microglia) around degenerative neurons is a common pathological feature of various neurological disorders including radiculopathy. Microglia exhibit a common, long-term response to a wide range of stimuli that threaten physiological homeostasis. This response includes changes in morphology, gene expression, function and number. Peripheral nerve injury leads to dramatic activation of microglia within the spinal dorsal horn [11]. Microglia activation in the spinal cord progresses through a hypertrophic morphology, with thickened and retracted processes and an increase in cell number. These criteria are immunohistochemical markers for assessing the activation state of microglia *in vivo* and among them, the change in cell number is the most prominent event [12]. Peripheral nerve injury increases the number of dorsal horn microglia by two to four fold [13-17].

Lumbar disc herniation occurs mostly in the spinal canal, because of injury proximal to the dorsal root ganglion (DRG). However, sometimes we face a specific type of radiculopathy, in which the percentage of lumbar disc herniation in the far lateral zone was 4.4–11.7% [18-20]. But the spinal nerve mechanisms around the DRG seem to be obscure, with little known about the degrees of radiculopathy injured at the DRG and proximal or distal to the DRG. Radiculopathy is an important and largely unresolved medical problem that requires further research into the etiological factors, to determine the correct diagnosis.

The purpose of this study was to examine the degrees of radiculopathy following injury at the DRG and proximal or distal to the DRG using different points of mechanical sensitivity, immunohistochemistry and *in vivo* patch-clamp recordings.

Results

Mechanical sensitivity

We counted the numbers of withdrawal reflexes in response to a sequential series of 10 tactile stimulations to the plantar surface of the ipsilateral (nerve root injured) hind paw using a 10 g von Frey filament. As rats rarely responded to the mechanical stimuli prior to surgery, the elevated behavioral responses evident after surgery were defined as allodynia. Behavioral tests were performed 7 days (7.8 ± 2.1 days, 220.5 ± 21.6 g) after surgery.

The number of withdrawal reflexes was 0.3 ± 0.2 times for group A (n = 10), 1.1 ± 0.5 times for group B (n = 10), 3.9 ± 0.5 times for group C (n = 10), 7.9 ± 0.5 times for group D (n = 10) and 6.2 ± 0.3 times for group E (n = 10). The number of withdrawal reflexes in the sham group (B) was not significantly increased compared with that in the normal group (A). While the rats in the nerve injury groups (C, D, and E) were significantly more sensitive compared with the rats in the sham groups (Student's *t* test, $P < 0.001$). The rats in group D were the most hypersensitive in the operated group, followed by groups E and C ($P < 0.001$) [Figure 1B].

Immunohistochemistry

We used a polyclonal antiserum directed against the ionized calcium-binding adapter molecule 1 (Iba1) to investigate whether microglia was activated and increased in the spinal dorsal horn 7 days after the surgery (208.4 ± 21.7 g) [Figure 2A]. We counted the number of microglia in laminas I–II of the L5 segment.

The number of activated microglia evident was 77.2 ± 2.5 for group A (n = 5), 80.0 ± 2.1 for group B (n = 5), 202.4 ± 8.0 for group C (n = 5), 354.6 ± 8.1 for group D (n = 5) and 292.1 ± 6.6 for group E (n = 5). There was no significant difference between groups A and B. The number of activated microglia was significantly increased in the nerve injury groups compared with the sham group ($P < 0.001$). The activated microglia seen in the nerve injury groups (C, D, E) developed at the superficial dorsal horn. The number of activated microglia was most significant in group D, followed by groups E and C ($P < 0.001$) [Figure 2B].

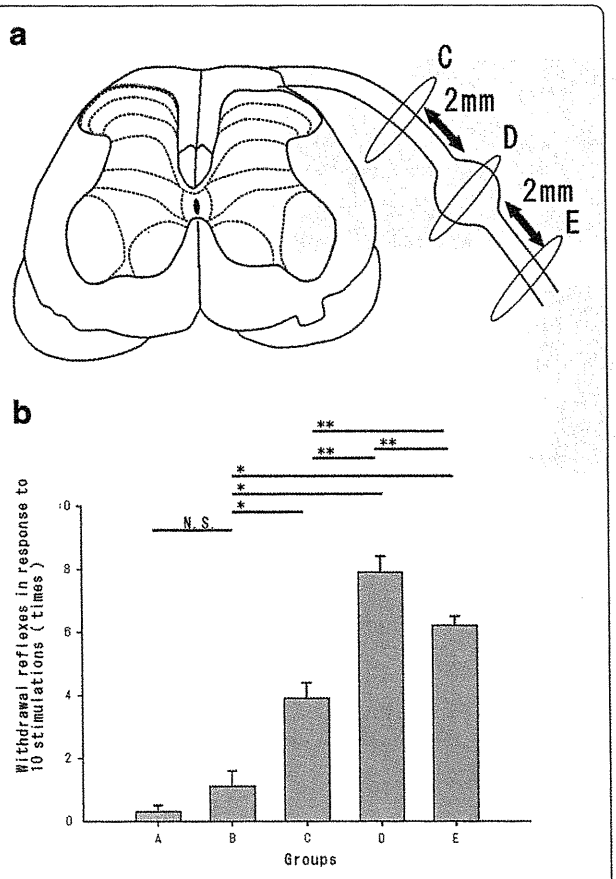

Figure 1 *A*. Schematic diagram of the radiculopathy rat model from the L5 nerve to the spinal cord: The L5 nerve was ligated at 2 mm proximal to the DRG (group C), at the DRG (group D), at 2 mm distal to the DRG (group E) by a microscope at 5× magnification. *B*. Withdrawal reflexes to 10 stimulations of a 10 g von Frey filament: The withdrawal threshold was a significantly different for nerve injury distal to the DRG compared with injury proximal to the DRG. There were no significant differences in the number of withdrawal reflexes between normal group A and the sham group B. The nerve injury groups (C, D, E) were more sensitive than the sham group (*$P < 0.001$), with significant differences between groups C, D and E (**$P < 0.001$).

In vivo patch-clamp recordings

Rats (218.4 ± 23.5 g n = 45) developed mechanical hypersensitivity approximately 7 days (7.6 ± 2.4 days) after surgery. A rat spinal cord preparation could be maintained in a stable condition for over 12 hours, which was equivalent to previous patch-clamp experiments using an artificial ventilator. Whole-cell patch-clamp recordings were performed in 50 SG neurons from the L5 segmental level of the spinal cord. All SG neurons were recorded at a holding potential (V_H) of −70 mV, where no inhibitory postsynaptic currents (IPSC) were observed [Figure 3A].

The average frequencies of excitatory postsynaptic currents (EPSC) were recorded in laminas I–II of the L5 segmental area. The frequencies of EPSC were 9.0 ± 1.4 Hz for group A (n = 10), 9.4 ± 1.3 Hz for Group B (n = 10), 14.6 ± 1.7 Hz for Group C (n = 10), 19.2 ± 2.0 Hz for Group D (n = 10), 17.3 ± 2.1 Hz for Group E (n = 10). The frequencies of EPSC in the nerve injury groups (C, D, E) were significantly increased compared with the sham group ($P < 0.001$). Interestingly, there were significant differences in the frequencies of EPSC between groups C, D and E ($P < 0.001$ and $P < 0.05$, respectively) [Figure 3B].

The amplitudes of EPSC were 12.3 ± 0.6 pA for group A (n = 10), 14.4 ± 1.0 pA for group B (n = 10), 19.8 ± 1.6 pA for group C (n = 10), 37.7 ± 2.2 pA for group D (n = 10) and 28.3 ± 2.4 pA for group E (n = 10). No significant difference in mean amplitudes of EPSC was observed between groups A and B. There were significant differences between groups B and C ($P < 0.05$), B and D ($P < 0.001$) and B and E ($P < 0.001$). Finally, there were significantly differences in mean amplitudes in C, D and E ($P < 0.001$) [Figure 3C].

Discussion

Several studies have investigated different types and degrees of nerve root or spinal nerve injuries [11,21]. Lesions close to the DRG produce more apoptosis when compared with lesions more distal to the DRG [22]. However, there was no report to compare the degrees of radiculopathy injured proximal or distal to the DRG. We investigated the degrees of radiculopathy following nerve injury via nerve ligation at an equal distance (2 mm proximal or distal) to the DRG. The degrees of radiculopathy were assessed using different points of mechanical sensitivity, immunohistochemistry and *in vivo* patch-clamp recordings.

Mechanical allodynia was observed at the plantar surface of the ipsilateral (nerve root injury site) hind paw at 7 days after surgery. The withdrawal threshold to von Frey stimulation in the nerve injury groups decreased compared with the sham model rats. Our behavioral data were consistent with the previous studies that showed development of maximum allodynia to occur at around 7 days post-injury in a rat model of nerve injury [23,24]. Interestingly, there was a significant difference in withdrawal threshold between the proximal and distal nerve injury to the DRG in this study.

Resting microglia (in the normal state) act as sensors for stimuli that threaten physiological homeostasis, including CNS trauma, ischemia, infection and neurodegeneration. Once activated by these stimuli, microglia undergo a common, series of progressive changes in morphology, function and number [13,25], which have been implicated in inducing central sensitization of spinal neurons [26]. ATP [27], substance P [28] and glutamate [29] are released in high amounts during central sensitization and participate in its induction and activate microglia [13,25], so that the sensitization of dorsal horn neurons may also stimulate microglia, which become further activated, establishing a

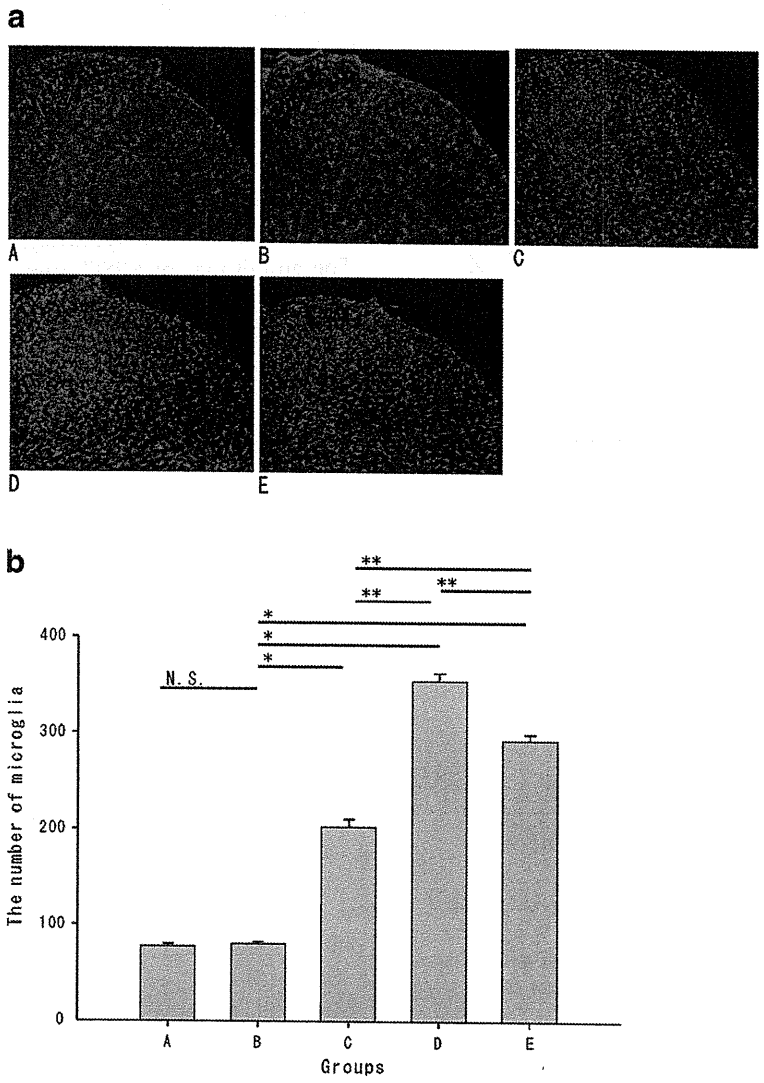

Figure 2 *A.* **Iba1 positive microglia in laminas I–II of the injured L5 segmental level: Activated microglia in the nerve injury groups (C, D, E) were observed, compared with the normal (A) and sham group (B).** *B.* The total number of microglia in laminas I–II of the injured L5 segmental level : There was no significant difference in the number of activated microglia between groups A and B. The nerve injury groups (C, D, E) were more sensitive than the sham group (*$P < 0.001$), with significant differences between C, D and E (**$P < 0.001$).

feed-forward cycle. Therefore, microglia is closely associated with the mechanisms of radiculopathy, with the number of activated microglia acting as an index for radiculopathy [13]. In this study, we show an approximate fourfold increase in microglia activation when compared with sham rats after surgery. Results consistent with previous studies, which found nerve injury to cause a two- to four-,fold increase in the number of microglia in the dorsal horn [13-17]. Interestingly, we show the number of microglia in rats injured distal to the DRG was significantly increased when compared with rats injured proximal to the DRG, consistent with the mechanical sensitivity results in the behavioral study. Together, these results indicate a difference in the degree of radiculopathy at distinct levels of nerve injury.

Microglia is also closely associated with neurons and astrocytes. Astrocytes have a more direct and active role in glutamatergic synapse function by releasing glutamate [30], releasing modulatory substances [31] and expressing functional N-Methyl D-Aspartate (NMDA) receptors [32]. NMDA receptors are activated by the wind-up phenomena, which is central pain sensitization caused by repeated stimulation of peripheral nerve fibers, leading to stimulation of C-fibers and a progressively increasing electrical response in the corresponding superficial dorsal horn. The mechanism underlying this phenomenon involves the release of glutamate by these pathologically sensitized C-fibers. The glutamate interacts with the postsynaptic NMDA receptors, which aids the sensitization of the dorsal

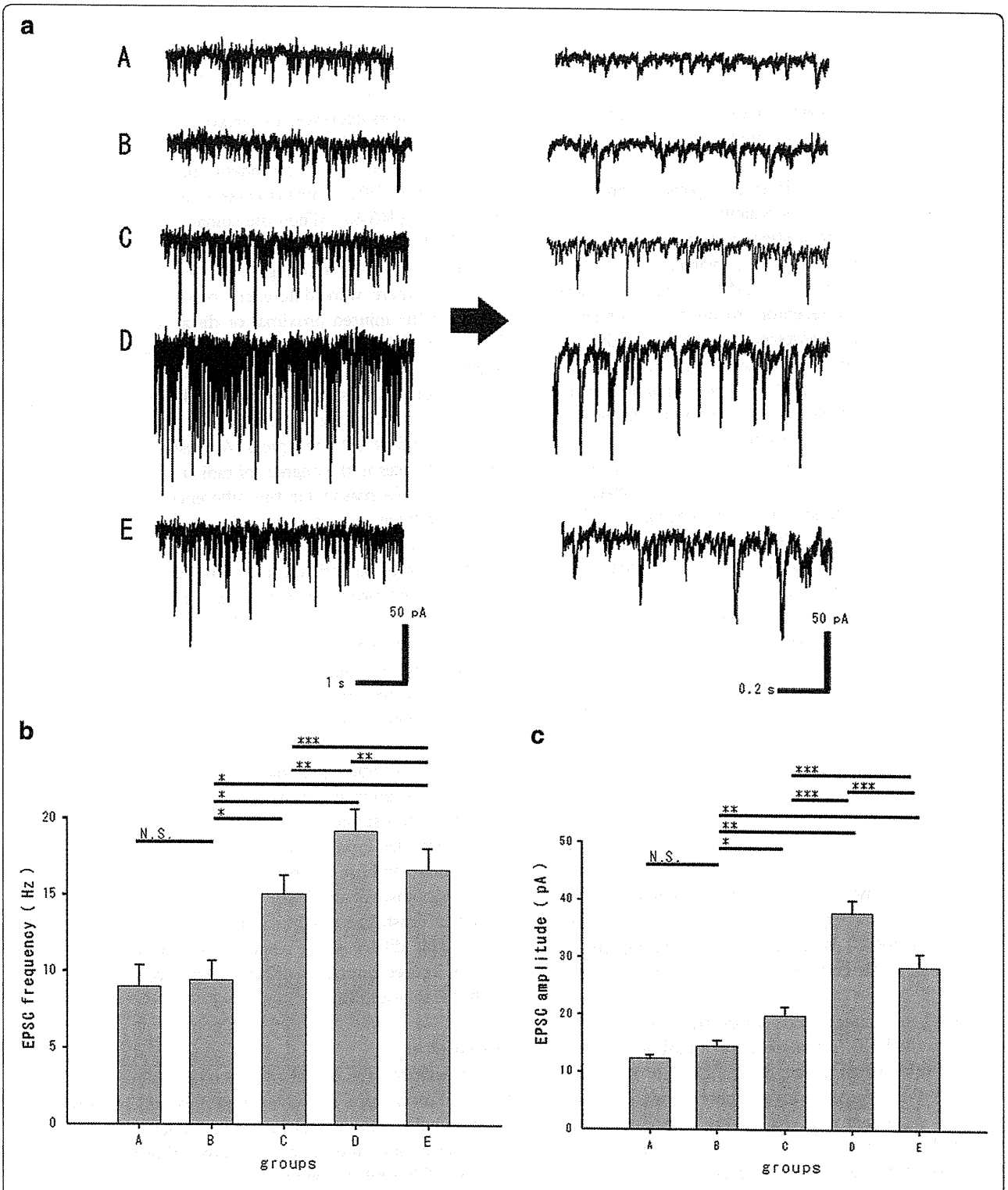

Figure 3 *A. In vivo* patch clamp data: EPSC were recorded at the SG of the injured L5 segmental level. All SG neurons were recorded at a holding potential (V_H) of −70 mV, where no IPSC were observed. *B.* The average frequencies of EPSC in laminas I–II of the L5 segmental level: No significant difference in EPSC frequency was shown between groups A and B. The frequencies of EPSC in nerve injury group (C, D, E) were significantly increased compared with the sham group (*$P < 0.001$) and interestingly there were significant differences between groups C, D and E (**$P < 0.001$ and ***$P < 0.05$, respectively). *C.* The average amplitudes of EPSC in laminas I–II of the L5 segmental level: No significant difference in the mean amplitudes of EPSC was observed between groups A and B. There were significant differences in mean amplitudes of EPSC between the nerve injury groups (C, D, E) and the sham group (B) (*$P < 0.05$ and **$P < 0.001$, respectively) as well as significant differences between groups C, D and E (**$P < 0.001$).